Trace-gas detection in ambient air with a thermoelectrically cooled, pulsed quantum-cascade distributed feedback laser

Anatoliy A. Kosterev, Frank K. Tittel, Claire Gmachl, Federico Capasso, Deborah L. Sivco, James N. Baillargeon, Albert L. Hutchinson, and Alfred Y. Cho

A pulsed quantum-cascade distributed feedback laser operating at near room temperature was used for sensitive high-resolution IR absorption spectroscopy of ambient air at a wavelength of ~8 μm. Near-transform-limited laser pulses were obtained owing to short (~5-ns) current pulse excitation and optimized electrical coupling. Fast and slow computer-controlled frequency scanning techniques were implemented and characterized. Fast computer-controlled laser wavelength switching was used to acquire second-derivative absorption spectra. The minimum detectable absorption was found to be 3×10^{-4} with 10^5 laser pulses (20-kHz repetition rate), and 1.7×10^{-4} for 5×10^5 pulses, based on the standard deviation of the linear regression analysis. © 2000 Optical Society of America
OCIS codes: 140.5960, 280.3420, 300.6320, 010.1280.

1. Introduction

The detection and quantification of trace gases in ambient air are of considerable importance for a number of applications, such as environmental monitoring, combustion diagnostics, and atmospheric chemistry. Precise, selective, and fast concentration measurements can be accomplished with IR absorption spectroscopy, because almost all molecules have strong absorption bands in the mid-IR region (2–20 μm). To realize the potential of this method, a tunable narrow-linewidth mid-IR source is necessary. Fabry–Perot lead-salt diode lasers have been the standard choice for use in this spectral region. Recently developed quantum-cascade lasers with distributed feedback[1] (QC-DFB) combine reliable single-frequency operation with high optical power and ease of handling. These features should lead to their wide adoption for spectroscopy (especially monitoring) applications throughout the mid-IR spectral region once they become commercially available. Already several high-resolution and high-sensitivity absorption spectroscopy measurements with QC-DFB lasers have been reported.[2–7] A potentially important property of QC lasers is that they can be operated without cryogenic cooling, to and above room temperature. This ability is of considerable value for many potential applications. Room-temperature operation, however, is possible only with a pulsed current excitation of typically ≤100-ns short pulses and a low (~1%) duty cycle and is accompanied by frequency chirping. Absorption spectroscopy with such pulsed QC-DFB lasers near room temperature has been reported in Refs. 6 and 7. Here we report on the further development of techniques for high-sensitivity laser absorption spectroscopy with thermoelectrically cooled QC-DFB lasers. The utility of these techniques is demonstrated by CH_4 and N_2O concentration measurements in ambient air.

2. Experimental Details

A schematic of the configuration of the pulsed QC-DFB laser-based gas sensor is shown in Fig. 1. A QC-DFB laser designed for pulsed operation at ~8 μm near room temperature was mounted on a three-stage thermoelectric unit inside compact evacuated housing (75 mm × 75 mm × 75 mm). The thermoelectric unit was driven by a temperature controller (Wavelength Electronics LFI-3751) communicating
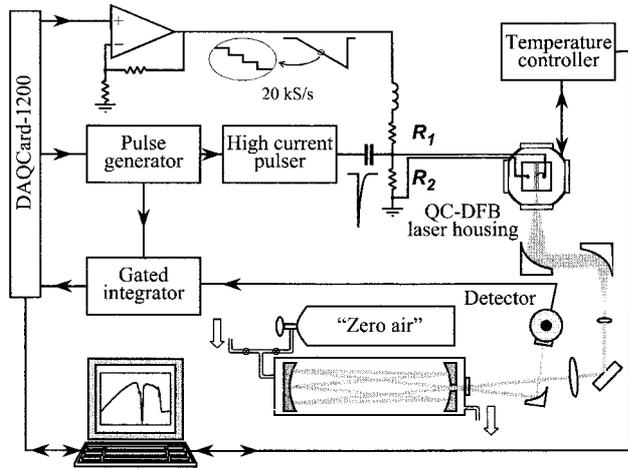
Fig. 1. Experimental arrangement for absorption spectroscopy with a pulsed QC-DFB laser. The laser is mounted on a thermoelectric cooler in an evacuated housing.
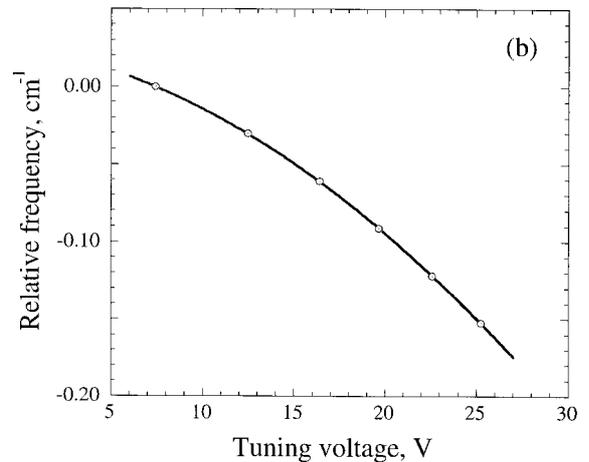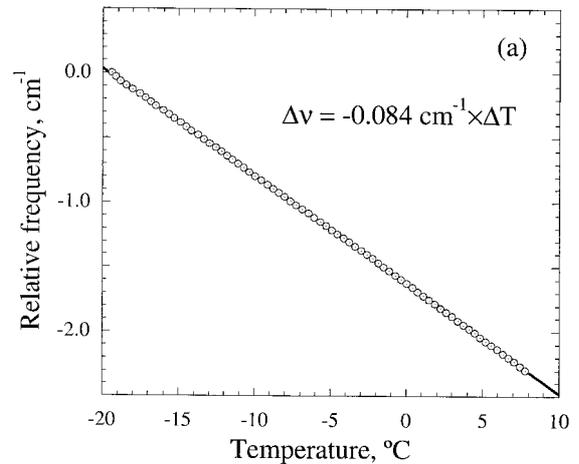

Fig. 2. Laser frequency: tuning (a) with temperature and (b) with a computer-controlled voltage applied to the resistor R_1 (shown in Fig. 1). The circles show the positions of the etalon fringes used for calibration.

with a laptop computer through an RS232 serial communication port. The temperature of the QC-DFB laser could be varied from -40 °C to above room temperature. In practice the laser temperature was usually kept below $+6$ °C because of a rapid decrease in laser power, an increase in threshold current, and the appearance of mode instabilities at higher temperatures. The laser light was collected and shaped into a narrow parallel beam by two off-axis parabolic mirrors and an uncoated BaF_2 lens. An additional lens with $f = 500$ mm was used to focus the beam on the entrance aperture of a 100-m path-length multipass cell (New Focus Model 5612). To obtain absorption spectra, a zero-air rapid background subtraction technique[8] was employed: The spectrum of nonabsorbing ultrapure nitrogen was subtracted from the spectrum of the gas sample being studied. The required rapid gas exchange was obtained by use of a pressure controller in combination with an electromagnetically actuated three-way valve. After exiting the multipass cell, the IR radiation was collected with a small off-axis parabolic mirror and detected with a liquid-nitrogen-cooled photovoltaic HgCdTe detector with a built-in preamplifier (20-MHz bandwidth). A Peltier-cooled detector could have been used at the cost of 1 order of magnitude of sensitivity. The detector signal was measured with a gated integrator (Stanford Research Systems SR-250) and a 12-bit data acquisition card (DAQC) (National Instruments DAQCard-1200) with a laptop computer. An integration window of 15 ns was set to integrate the signal at a peak of $\sim$35-ns FWHM detector response. The useful signal was separated in time from any interfering scattered light owing to a 330-ns delay of the laser pulse in the multipass cell.

Short current pulses ($\sim$5-ns FWHM) were supplied to the laser through a low-impedance stripline. This short duration was selected because we found that the laser linewidth decreased when the pulse dura-

tion varied from 50 to 7 ns. The pulse repetition rate was limited to 20 kHz by the minimum acquisition time of the gated integrator. A variable pedestal of computer-controlled subthreshold current was added to each pulse, enabling fast wavelength tuning. A similar frequency scanning technique with an analog subthreshold linear current ramp has been described in Refs. 6 and 7. In our experiments the current offset was created by applying an amplified computer-synthesized voltage from the digital-to-analog converter of the DAQC to the laser through a decoupling resistor, $R_1 = 50$ Ω. Computer control adds flexibility to the device architecture, enabling arbitrary waveforms to be applied. We found that when the subthreshold current exceeded 230 mA, the laser operation became unstable. This effect limited fast laser tunability to $\sim$0.23 cm^{-1}. Slow laser frequency tuning was performed by changing the laser temperature. Variation of the laser temperature from -25 to $+5$ °C allowed tuning in a spectral range from $\sim$1255.5 to 1258.0 cm^{-1}. Frequency calibration curves for slow and fast laser scans are shown in Figs. 2(a) and 2(b), respectively. These data were

obtained by using the interference fringes produced by two air-separated uncoated ZnSe surfaces. The slow scan is linear with a coefficient of -0.084 cm^{-1} °C. The solid line in Fig. 2(b) shows a third-order polynomial fit.

Initial experiments indicated that the spectral shape of the pulsed QC-DFB laser radiation exhibited a sharp peak and a broad lower-frequency tail, sometimes with oscillations. The portion of the energy in the tail increases with excitation laser current and especially with the duration of current pulses, being very pronounced when the pulses are longer than 10 ns. We attribute this effect to the heating of the QC-DFB lasers by the excitation current pulse. The oscillations are most likely due to imperfect coupling of the laser to the pump pulse source and related electric ringdown. A compact pulser module with a fixed pulse duration of ~5 ns was used in the present laser spectrometer design to minimize the heating-related laser frequency chirp. This module produces electric pulses with a sharp rising front and an exponentially decaying tail. It was connected to the laser with a high-frequency stripline. A coupling resistor, $R_2 = 7.9$ Ω, was connected to the stripline to suppress electrical oscillations in the circuit. The correct choice of R_2 is critical for the spectral properties of the QC-DFB laser radiation. The use of this resistor was found to ensure a significantly smaller laser linewidth (2×) at the same or even higher laser power levels.

3. Results and Discussion

Both fast-scan and slow-scan techniques were investigated for acquiring absorption spectra. An approximate absolute frequency calibration (laser frequency as a function of temperature) was made before the trace-gas concentration measurements. We accomplished this by measuring the transmission of a 3-cm-long reference cell filled with 2 Torr of CH$_4$ while we varied the laser temperature.

A. Fast Frequency Scanning

In a fast-scan data-acquisition mode, the laser temperature was chosen first so that the laser operated near an absorption line of interest. The pulse generator was triggered by the DAQC, and a computer-synthesized voltage pedestal was applied to each short high-current pump pulse. The intensity of each laser pulse was individually measured after the multipass cell, digitized, and stored in the computer memory. Each scan consisted of 512 data points, limited by the available onboard DAQC memory. The scans were repeated continually, and the data were averaged until a preset number of scans was reached.

The laser frequency exhibits an essentially nonlinear dependence on the offset voltage applied to the stripline as seen in Fig. 2(b). This nonlinearity was taken into account, and the voltage waveform was corrected so that the laser frequency varied linearly with the data point number (hence with time) during each scan. If the relative laser frequency ν ($\nu = 0$ at $N = 0$, where N is a data point number) depends on
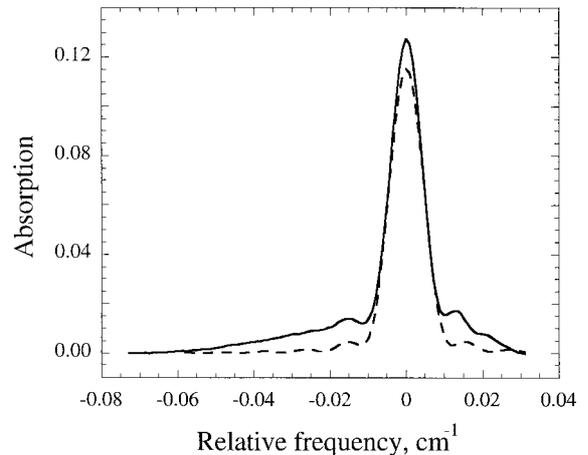

Fig. 3. Solid line, acquired envelope of the CH$_4$ absorption line at 1256.602 cm^{-1}; dashed line, simulated envelope computed as a convolution of the Doppler-limited absorption line with a Fourier transform of a 3.1-ns-long rectangular pulse. The experimental data were obtained with a 3-cm-long gas cell filled with 1.25 Torr of CH$_4$.

the applied voltage as $\nu = f(U)$ and the voltage is related to the data point number as $U = g(N)$, a desired linear relation of frequency and data point numbers can be expressed as

$$\nu = f(U) = f[g(N)] = \nu_{\max} \times N/N_{\max},$$

which yields

$$U = g(N) = f^{-1}(\nu_{\max} \times N/N_{\max}).$$

Using this equation, we numerically calculated the function $g(N)$ from the data in Fig. 2(b), and the resulting array of 512 points was loaded into computer memory for subsequent voltage synthesis. Further calibration based on interference fringes confirmed the linear dependence of frequency versus the data-point number for the total scan range of 0.22 cm^{-1}. All the data for the fast-scanning mode were obtained with this linearization technique.

To characterize the spectral properties of the laser pulses, the laser temperature was set to -8.5 °C to enable a fast scan across the CH$_4$ absorption line at 1256.601 cm^{-1}. The laser pulses were detected after they passed through a 3-cm-long cell that was alternately filled with 1.25 Torr of CH$_4$ and evacuated. The measured absorption spectrum is shown in Fig. 3 as a solid curve. The area under the acquired absorption curve was found to be 15% less than an integrated absorption of this line as predicted from the HITRAN spectroscopic database. This inconsistency is due to the ambiguity in the baseline shape because of interference fringes created by the plane–parallel windows of the absorption cell. The baseline ambiguity makes it difficult to measure accurately the area under the broad pedestal observed in the spectrum. Nevertheless, it is evident that this spectral pedestal is asymmetric. This fact points to the presence of a frequency chirp, because the Fourier transform of any monochromatic pulse is
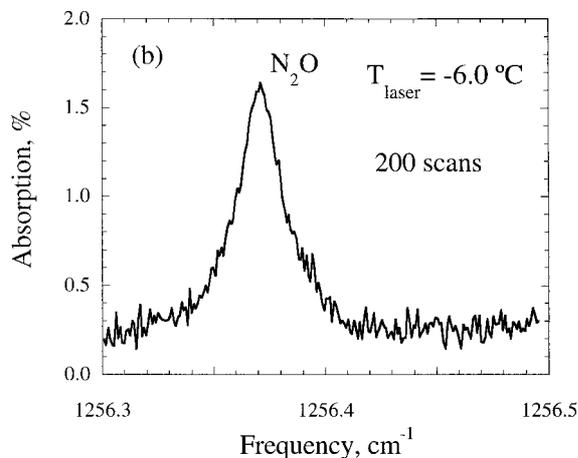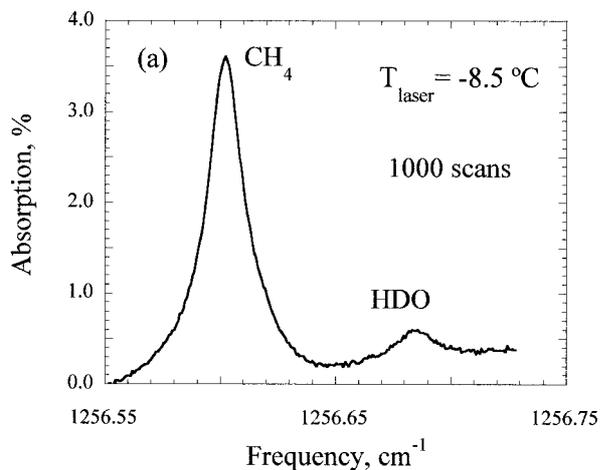
Fig. 4. Absorption spectra of ambient air in a 100-m path-length multipass cell obtained with a linearized fast frequency scanning technique: (a) laser temperature set to -8.5 °C; (b) laser temperature set to -6.0 °C. The pressure in the cell is 85 Torr.

symmetric. However, the pulse spectrum has a narrow peak that can be approximated by a Fourier transform of a rectangular pulse that is $\tau = 3.1$ ns long. A convolution of the function $g(\nu) = \text{const} \, \sin^2(\pi\nu\tau)/\nu^2$ with an absorption line shape is shown by the dashed curve in Fig. 3; $g(\nu)$ is normalized so that the difference between peak and dip positions is the same as for the measured spectrum. A rectangular pulse shape is a good approximation to the actual laser pulse, because the laser starts to emit only after the injected current reaches the lasing threshold and the derivative of current cannot instantly change its sign on top of the current pulse. From a comparison of areas under the solid and the dashed curves we estimate that the portion of energy in the transform-limited part of the spectrum is 75%. The FWHM of the narrow spectral peak is 9.5×10^{-3} cm^{-1}, or 290 MHz. The acquired laser line shape describes the instrument function of the laser spectrometer and was used to process the absorption spectra described below. The achieved spectral resolution cannot be significantly improved for this kind of laser because of the Fourier-transform limitation
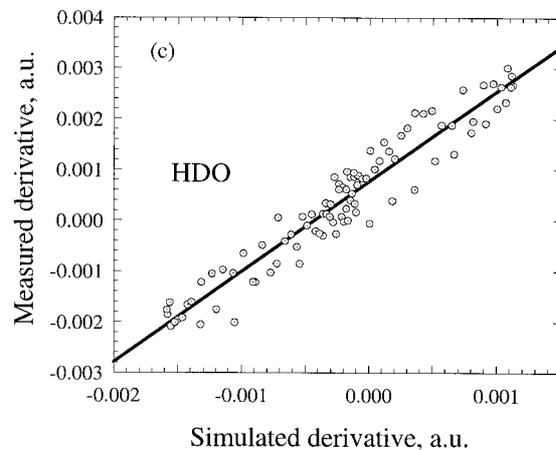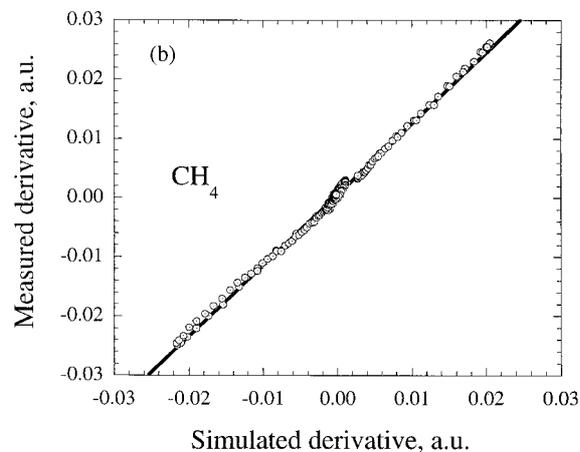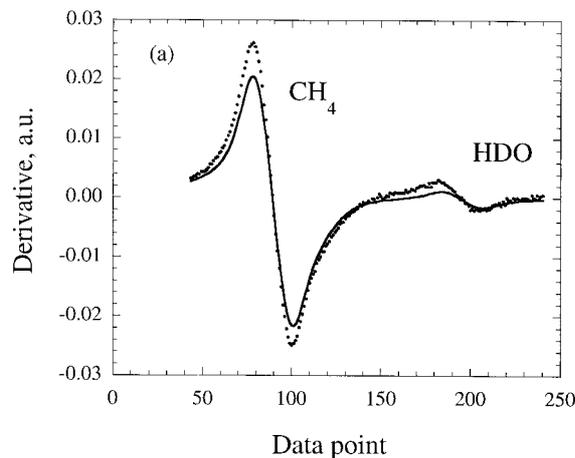
Fig. 5. CH$_4$ and HDO concentrations obtained from fast-scan measurements: (a) Solid line, simulated first-derivative spectrum of standard air, with the laser line shape taken into account; dotted line, acquired data after calculation of a numerical derivative. (b) Linear regression analysis of the data above for the CH$_4$ line. (c) Same analysis for the HDO line.

for shorter pulses and significant frequency chirping for longer pulses. Further narrowing of the laser linewidth requires lasers with decreased thermal dissipation.

We applied the described data-acquisition technique to detect CH$_4$ and N$_2$O in ambient air by using

Table 1. Measurements of Trace-Gas Concentrations by Linear Regression Analysis of Fast-Scan Data

Parameters and Results	Detected Molecular Species		
	CH_4	HDO	N_2O
Concentration assumed in simulations (ppm)	1.7	2.408	0.32
Simulated peak absorption (%)	4.58	0.29	2.15
Number of scans	1000	1000	200
Linear regression slope	1.195 ± 0.005	1.78 ± 0.05	0.998 ± 0.014
Resulting concentration (ppm)	2.032 ± 0.009	4.28 ± 0.12	0.319 ± 0.004

a 100-m path-length optical multipass cell. The laser temperature was set to -8.5 °C to detect a CH_4 absorption line at 1256.601 cm^{-1} and to -6.2 °C to detect an N_2O absorption line at 1256.371 cm^{-1}. Examples of acquired spectra are shown in Fig. 4. The weaker line in Fig. 4(a) is due to HDO absorption at 1256.684 cm^{-1}. Both spectra were acquired at 85-Torr air pressure in the multipass cell. The baseline (no-absorption line) of the acquired data exhibit some slow variations despite use of the zero-air technique. We attribute this to acoustic vibrations of the optical table that lead to small displacements of the laser beam. This was confirmed by a spectral analysis of the noise, which indicated a strong 90-Hz component that correlates with optical table vibrations. A single cycle of data acquisition (510 laser pulses) corresponds to a frequency of 20 kHz/510 $\approx$ 40 Hz, in accord with the conclusion that acoustic noise causes the variations in the observed baseline.

To determine the concentrations of absorbing species, the following procedure was applied:

(1) The acquired spectra were numerically differentiated by subtracting a shifted array of the same data. This resulted in suppressing the baseline offset and slow baseline variations [Fig. 5(a)].

(2) The absorption of air in the cell at 85 Torr was simulated by the HITRAN database, and this spectrum was convolved with the laser spectrometer instrument function shown in Fig. 3.

(3) The resulting simulated absorption spectrum was numerically differentiated as in step (1).

(4) Linear regression analysis was applied to define the ratio of absorption in the experimentally observed spectrum to the corresponding absorption in the simulated spectrum [Figs. 5(b) and 5(c)]. This ratio was obtained as a slope of the linear fit.

This algorithm was applied to determine the concentrations of CH_4, HDO, and N_2O in air. The results are listed in Table 1. The methane concentration is in good agreement with previous measurements in the Houston area.[9] Absorption of HDO, when compared with the HITRAN data, gives a relative humidity of 49%, which is lower than the hygrometer readings of 60%. However, the isotopic abundance of deuterium assumed in this database is 10–30% higher than in natural atmospheric water vapor, and this explains the deviation of the humidity calculated from the HDO absorption and the hygrometer read-

ings.[10] The concentration of N_2O was found to match the standard air value. The calculated standard deviation of the fitting line slope for all three absorption lines corresponds to a minimum detectable absorption of 3×10^{-4} when averaging over 200 scans (10^5 laser pulses at a 20-kHz repetition rate, 15 s of total data-acquisition time including software delays) and 1.7×10^{-4} for 1000 scans.

B. Slow Frequency Scanning

To cover a larger frequency range in a single laser scan, slow temperature scanning is necessary. The simplest technique of acquiring such spectra consists of a slow continuous change in the laser temperature while absorption of the laser pulses in the gas sample is periodically measured. When such measurements were carried out it was found that low-frequency noise is present in the acquired spectra with a peak-to-peak magnitude corresponding to ~1% absorption. This noise was due mainly to acoustic vibrations of the laboratory table. (In particular, a strong 90-Hz component was found.) To eliminate the low-frequency noise, we applied a modification of the wavelength-modulation technique. Our method is illustrated in Fig. 6. A sequence of 510 laser pulses with a repetition rate of 20 kHz was
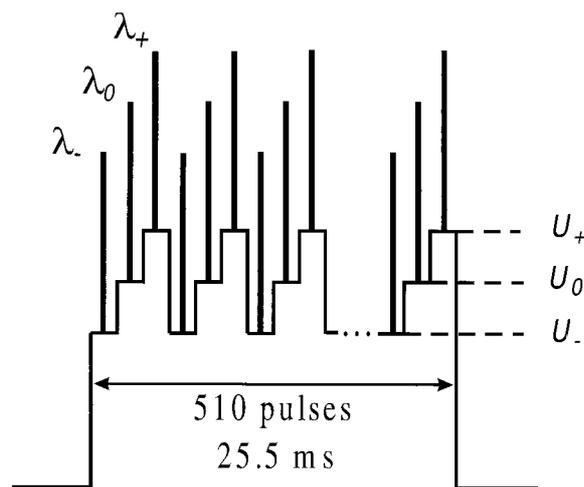

Fig. 6. Schematic of computer-controlled wavelength cycling for a pulsed QC-DFB laser. The steps show a subthreshold current (controlled by the computer-synthesized voltage U_i) added to the short laser excitation pulses represented as spikes. The laser wavelength cycles through three temperature-dependent values λ_i.
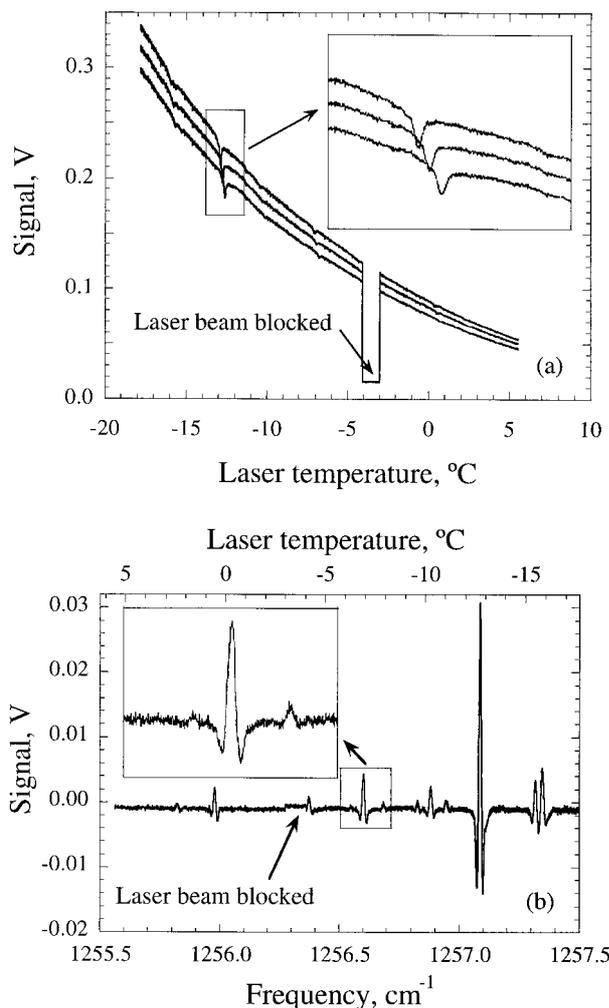
Fig. 7. Modified wavelength modulation spectroscopy: (a) IR detector signal simultaneously acquired at three laser wavelengths; (b) resulting second-derivative signal. Inset shows (left to right) weak H_2O, CH_4, and HDO absorption lines. The two lines to the right on the main plot correspond to N_2O and HDO absorption. The second-derivative signal is not normalized for changing laser power. The data are acquired at 50 Torr of air in the multipass cell.

periodically generated, and pedestals of software-selectable voltages, U_0, U_+, or U_-, were added cyclically to each subsequent electrical excitation pulse. Such an alternating offset resulted in switching the laser wavelength among three (close) values, and the data were separately collected and averaged over $510/3 = 170$ pulses for each wavelength. So, this 25.5-ms-long train of 510 pulses resulted in almost simultaneous laser pulse attenuation measurements at three different temperature-dependent wavelengths. When repeated continually, such measurements provide three arrays of data, $S_0(T)$, $S_+(T)$, and $S_-(T)$ [Fig. 7(a)], where S is the IR detector signal. Differences $D(T) = S_+(T) - S_0(T)$ and $D^2(T) = S_+(T) + S_-(T) - 2S_0(T)$ yield discrete analogs of the first and the second derivatives $\partial S/\partial \nu$ and $\partial^2 S/\partial \nu^2$, respectively. Low-frequency noise adds the same fluctuations to all three data arrays; therefore $D(T)$ and $D^2(T)$ are free of them. To obtain a high $D(T)$ and $D^2(T)$

without loss of resolution, voltage pedestals were chosen so that the frequency differences, $\nu_+ - \nu_0$ and $\nu_0 - \nu_-$, matched the half-width of an absorption feature, namely, ~ 0.012 cm^{-1} at a pressure of 50 Torr.

An example of a $D^2(T)$ spectrum of ambient air is shown in Fig. 7(b). This spectrum was derived from the set of data represented in Fig. 7(a) and was acquired at 50 Torr of air in the 100-m path-length multipass cell. The $D^2(T)$ signal was not normalized to the laser intensity, which increased almost 8.5 times from $+5$ to -25 °C. The noise did not depend noticeably on the temperature (and laser intensity) and also did not change when the laser beam was blocked. Separate measurements of the dark noise also revealed a match to the noise in a $D^2(T)$ signal. This confirms cancellation of the vibration-related fluctuations in the detected signal. It also means that fluctuations in energy of the laser pulses are negligibly small compared with detection noise.

A comparison of the signal-to-noise ratio in the $D^2(T)$ data to the known absorption of CH_4, H_2O, and HDO lines near 1256.6 cm^{-1} (-7 °C) showed that the detection limit of these measurements is 6×10^{-4} peak absorption. That compares with a minimum detectable absorption of 3×10^{-4} for 200 averaged fast scans. An estimate of the number of laser pulses N involved in the measurements of a single absorption line was made. An addition of uncorrelated fluctuations in quadrature when the derivative is calculated was also taken into account. This evaluation gave a four times lower N value for a slow scan than for a 200 times averaged fast scan. Hence the detection limit normalized to $\sqrt{N}$ is the same for fast and slow scans. The sensitivity for both modes of spectral measurements is limited by random errors of the measuring electronics (mainly by detector dark noise).

4. Conclusions

A laser spectrometer with an instrument function of 290 MHz based on a thermoelectrically cooled QC-DFB laser was developed. Computer control of the QC laser current allows fast 0.22-cm^{-1}-long linear laser frequency scans, or an alternative mode of operation permits the acquisition of second derivative absorption spectra for slow 2.5-cm^{-1}-long scans while low-frequency noise is suppressed. Concentration measurements of CH_4, N_2O, and HDO in ambient air were carried out. An absorption sensitivity of 1.7×10^{-4} was achieved.

References

1. F. Capasso, C. Gmachl, D. L. Sivco and A. Y. Cho, "Quantum cascade lasers," Phys. World **12,** 27–33 (1999); also F. Capasso, C. Gmachl, A. Tredicucci, A. L. Hutchinson, D. L. Sivco, and A. Y. Cho, "High performance quantum cascade lasers," Opt. Photon. News **10,** 32–37 (1999).

2. B. A. Paldus, C. C. Harb, T. G. Spence, R. N. Zare, C. Gmachl, F. Capasso, D. L. Sivco, J. N. Baillargeon, A. L. Hutchinson, and A. Y. Cho, "Cavity ringdown spectroscopy using mid-infrared quantum-cascade lasers," Opt. Lett. **25,** 666–668 (2000).

3. A. A. Kosterev, R. F. Curl, F. K. Tittel, C. Gmachl, F. Capasso, D. L. Sivco, J. N. Baillargeon, A. L. Hutchinson, and A. Y. Cho, "Methane concentration and isotopic composition measurements with a mid-infrared quantum-cascade laser," Opt. Lett. **24,** 1762–1764 (1999).

4. B. A. Paldus, T. G. Spence, R. N. Zare, J. Oomens, F. J. M. Harren, D. H. Parker, C. Gmachl, F. Capasso, D. L. Sivco, J. N. Baillargeon, A. L. Hutchinson, and A. Y. Cho, "Photoacoustic spectroscopy using quantum-cascade lasers," Opt. Lett. **24,** 178–180 (1999).

5. S. W. Sharpe, J. F. Kelly, J. S. Hartman, C. Gmachl, F. Capasso, D. L. Sivco, J. N. Baillargeon, and A. Y. Cho, "High-resolution (Doppler-limited) spectroscopy using quantum-cascade distributed-feedback lasers," Opt. Lett. **23,** 1396–1398 (1998).

6. K. Namjou, S. Cai, E. A. Whittaker, J. Faist, C. Gmachl, F. Capasso, D. L. Sivco, and A. Y. Cho, "Sensitive absorption spectroscopy with a room-temperature distributed-feedback quantum-cascade laser," Opt. Lett. **23,** 219–221 (1998).

7. D. Sonnenfroh, E. Wetjen, M. Miller, M. Allen, C. Gmachl, F. Capasso, A. L. Hutchinson, D. L. Sivco, J. N. Baillargeon, and A. Y. Cho, "Application of balanced detection to absorption measurements with quasi-cw QC lasers," OSA Trends in Optics and Photonics Series, Vol. 36, Laser Applications to Chemical and Environmental Analysis, Technical Digest, Postconference Edition (Optical Society of America, Washington, D.C., 2000), pp. 60–62.

8. A. Fried, S. Sewell, B. Henry, B. P. Wert, T. Gilpin, and James R. Drummond, "Tunable diode laser absorption spectrometer for ground-based measurements of formaldehyde," J. Geophys. Res. **102,** 6253–6266 (1997).

9. D. Richter, D. G. Lancaster, F. K. Tittel, "Development of an automated diode laser based multicomponent gas sensor," Appl. Opt. **39,** 4444–4450 (2000).

10. International Atomic Energy Agency/World Meteorological Organisation (Geneva) (1998), Global Network for Isotopes in Precipitation (The GNIP Database. Release 3, October 1999), http://www.iaea.org/programs/ri/gnip/gnipmain.htm.